

1 **Rockslides on limestone cliffs with sub-horizontal bedding in the southwestern calcareous**
2 **area, China**

3

4 Authors: Z. Feng¹, Y.P. Yin², B. Li¹, K. He³

5 1. Key Laboratory of Neotectonic Movement and Geohazard of MLR at Institute of

6 Geomechanics, Chinese Academy of Geological Science, Beijing 100081, China.

7 2. China Institute of Geo-Environment Monitoring, Beijing 100081, China

8 3. Chang'an University, Xi'an 710054, China

9 *. Correspondence to: B. Li. (libin1102@163.com, +86-010-88815022)

10

11 **Abstract:** Calcareous mountainous areas are highly prone to geohazards, and rockslides play an
12 important role in cliff retreat. This study presents three examples of failures of limestone cliffs
13 with sub-horizontal bedding in the southwestern calcareous area of China. Field observations and
14 numerical modeling of Yudong Escarpment, Zengzi Cliff, and Wangxia Cliff showed that
15 pre-existing vertical joints passing through thick limestone and the alternation of competent and
16 incompetent layers are the most significant features for rockslides. A “hard on soft” cliff made of
17 hard rocks superimposed of soft rocks is prone to rock slump, characterized by shearing through
18 the underlying weak strata along a curved surface and backward tilting. When a slope contains
19 weak interlayers rather than a soft basal layers, a rock collapse could occur from the compression
20 fracture and tensile split of the rock mass near the interfaces. A rock slide might shear through a
21 hard rock mass if no discontinuities are exposed in the cliff slope, and sliding may occur along a
22 moderately inclined rupture plane. The “toe breakout” mechanism mainly depends on the strength

23 characteristics of the rock mass.

24 **Key words:** cliff failure; sub-horizontal bedding; plane slide; toe splitting; rock slump; numerical
25 modeling

26

27 **1. Introduction**

28 The southwestern calcareous area of China covers a large area of $54.4 \times 10^3 \text{ km}^2$, and it is highly
29 prone to geohazards. Many multilayered carbonate rocks with sub-horizontal bedding have been
30 deeply cut by rivers during crustal uplift and form significant topographic relief in steep slopes
31 and cliffs. These sub-horizontal cliff slopes are usually dominated by two sets of sub-vertical
32 conjugate joints and are characterized by slightly folded or faulted to massive rock masses.
33 Rockslides from sub-horizontally bedded cliff failure and resulting catastrophes have occurred
34 widely and frequently in the southwestern calcareous area of China.

35 Considerable research on cliff failure has been conducted in similar areas around the world(Abele,
36 1994; Von, 2002; Rohn, 2004; Embleton, 2007; Ruff, et al., 2008; Palma, et al., 2012), such as the
37 North Calcareous Alps in Austria. It is believed that water, lithology, geological structure, and
38 karstification are of primary importance in triggering rockslides from cliff failure (Kay, et al.,
39 2006). These factors dominate the tearing and shearing failure mechanism of the rock masses and
40 joints, which are directly displayed in the consequent failure behavior of the cliff slopes. Types of
41 rockslides with different detachment mechanisms (slumps, plane slides, topples, and lateral
42 spreading) in sub-horizontally bedded cliffs with particular geological settings and triggering
43 mechanisms have been described by engineering geologists, e.g., the collapse of the Mt. Sandling
44 and Mt. Raschberg limestone towers had a complex failure sequence from lateral spread to

45 toppling followed by rock fall (Rohn, et al., 2004). In addition to lateral spreading, a cliff slope
46 with a geological formation of hard rock on a soft base may undergo the translational sliding or
47 slumping of slab-shaped blocks (Poisel, 2005). In addition, the karst process is an inevitable factor
48 in rockslide formation. Tectonic joints keep widening and extending to the deep of rock mass by
49 constant dissolution and disgregation of underground water, forming boundaries of perilous rocks
50 (Santo, et al., 2007). It is believe that karst plays an important role in rockslides from carbonate
51 mountains, especially for gently bedding-inclined slopes which are unfavorable to failure.


52 Active underground mining is widespread in the southwestern calcareous area of China. There is
53 the potential for damage to cliff faces and overhangs when mining activity occurs beneath cliffs.
54 This has been repeatedly shown to be true. Taking the Southern Coalfields of Australia as an
55 example, several types of cliff failure have been witnessed in the goaf area, although no
56 instabilities have been reported beyond the mining area (Kay, 2006). However, there is no
57 available and widely accepted model that can predict the failure susceptibility of steep slopes close
58 to mining. This is because of the complex interaction of factors influencing the stability of steep
59 slopes, which include geometry, geology, geological structure, environmental factors, and
60 technical mining parameters. An integrated method combining landslide science and mining
61 subsidence science is promising as a direction for future research.

62 This study focuses on the failure mechanisms of cliffs with sub-horizontal bedding in the
63 southwestern calcareous area of China and the recognition of these features in field investigations.
64 The three cases presented occurred during the last 10 years and caused great damage to both
65 human life and assets. Furthermore, post-failure behavior, such as rock avalanches and debris
66 flows, is not included in descriptions of failure mechanisms of steep slopes. The term “failure

67 mechanism” in this study particularly refers to the detachment mechanism of rock masses from the
68 cliff slope.

69

70 **2. Geological background**

71 The likelihood of rockslide instability in the southwestern calcareous  area is high, mainly
72 because of the local geological evolution. Tectonic movement during the Mesozoic was
73 characterized by compression and formed the area into a fold belt, mainly striking NNE.
74 Neotectonic uplift raised the thick carbonate rocks to high altitude and shaped the steep and folded
75 landforms.

76 Many layers of carbonate rocks were deposited from Permian until Triassic time, and were
77 interbedded with weak planes or soft strata. The carbonate rock masses possess great strength and
78 integrity; thus, they usually form steep slopes hundreds of meters high, e.g., the Three Gorges, if
79 there are no intercalated soft strata. Under these circumstances, slope movement is mainly
80 controlled by discontinuities such as weak interlayers, karst, and fissures. The thick carbonate
81 succession in the southwestern calcareous area of China contains multiple layers of weak shale
82 planes, including carbonaceous shale and pyrobituminous shale. The strength of the shale planes is
83 relatively low and significantly varies with the weathering process, from virgin rock to fractured
84 planes to argillated layers. The strength of carbonaceous shales sandwiched in the Lower Permian
85 limestone at Lianziya Cliff is low that the cohesion and internal friction angle are 0.08–0.39 MPa,
86 18°–21° and 0.06–0.078 MPa, 18°–19.8° for dry and saturated samples, respectively (Ding, et al.
87 1990). The weak interlayers play a significant role in mass movement. When soft strata underlie
88 hard rock, the yielding of the soft base may cause the uneven subsidence of the cap rock. Lateral

89 spreading and slumps with backward tilting are caused by this type of destabilization mechanism,
90 in which failure propagates uphill.

91 In the southwestern calcareous area of China, coal measures are common soft strata, accompanied
92 by thick carbonate sequences. Except for coal seams, the coal measures are usually composed of
93 associated interlayers of shale, carbonaceous shale, pyrobituminous shale, and bauxitic claystone.
94 Mining is active in these coal measures using the techniques of room and pillar mining and
95 longwall mining. The depth of cover ranges from dozens to hundreds of meters. It is believed that
96 underground mining activities can change the engineering geological conditions and reduce the
97 stability of cliffs (Tang, 2009; Altun, et al., 2010; Marschalko, et al., 2012; Lollino, et al., 2013), .
98 Cliff failures and the resulting catastrophes, examples of which are discussed below, are related to
99 underground mining.

100 Karstification is a significant factor when discussing the reasons for carbonate slope failure. It
101 particularly affects steeply inclined faults and tectonic joints and slowly widens the discontinuities
102 to create large open fractures, which foster rockslides (Santo et al., 2007; Parise, 2008). In
103 addition, the karstification process can cause a significant reduction in the mechanical properties
104 of the carbonate rock mass. This is very important for toe-constrained slides, which depend on the
105 strength of the rock mass at the toe. In some cases, the underground karst voids play the same role
106 as goaf, and cavern breakdown may also lead to landslides (White, et al., 1969; Parise, 2010).

107

108 **3. Failure mode**

109 Different types of rockslides have been observed in thickly and sub-horizontally bedded limestone
110 escarpments. Gently inclined bedding is unfavorable for large translational slides. Slide, collapse,

111 and slump slope failures are discussed below in detail to explain their mechanisms. Three
112 examples are given: the Yudong Escarpment, Zengzi Cliff, and Wangxia Cliff (Fig. 1).

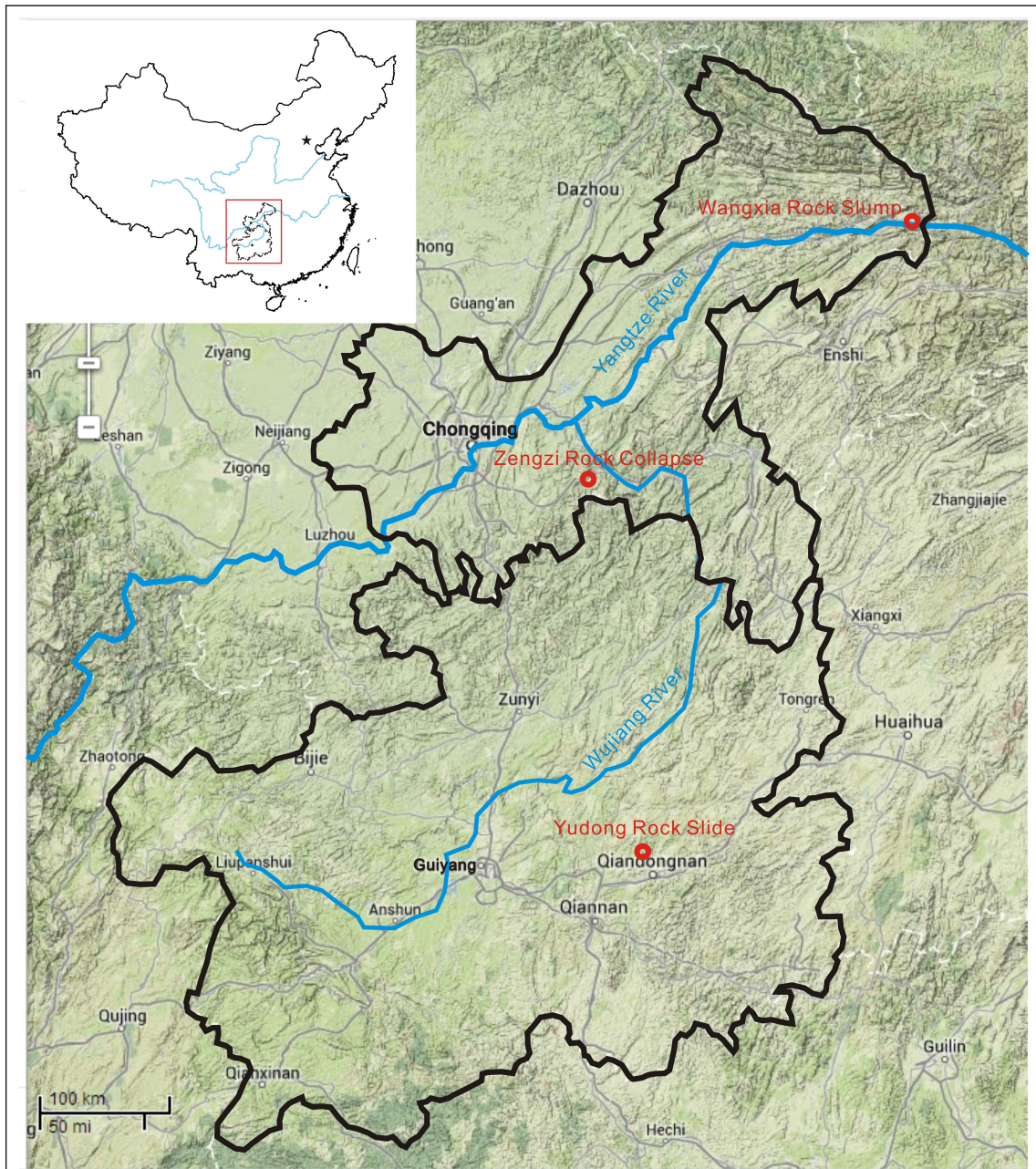


Fig. 1 Locations of three rockslides: Wangxia Rock Slump, Zengzi Rock Collapse, and Yudong

Rock Slide. 

113

114 **(1) Rock slide at the Yudong Escarpment**

115 On February 18, 2013, a rock slide occurred in Longchang County, Guizhou Province. The

116 mass movement is located in a high and steep bank of the Yudong River, close to an underground
117 mining area (Fig. 2). The S308 provincial road runs on the opposite bank of the river. The rock
118 slide buried several houses and five people beneath the escarpment and blocked the river.

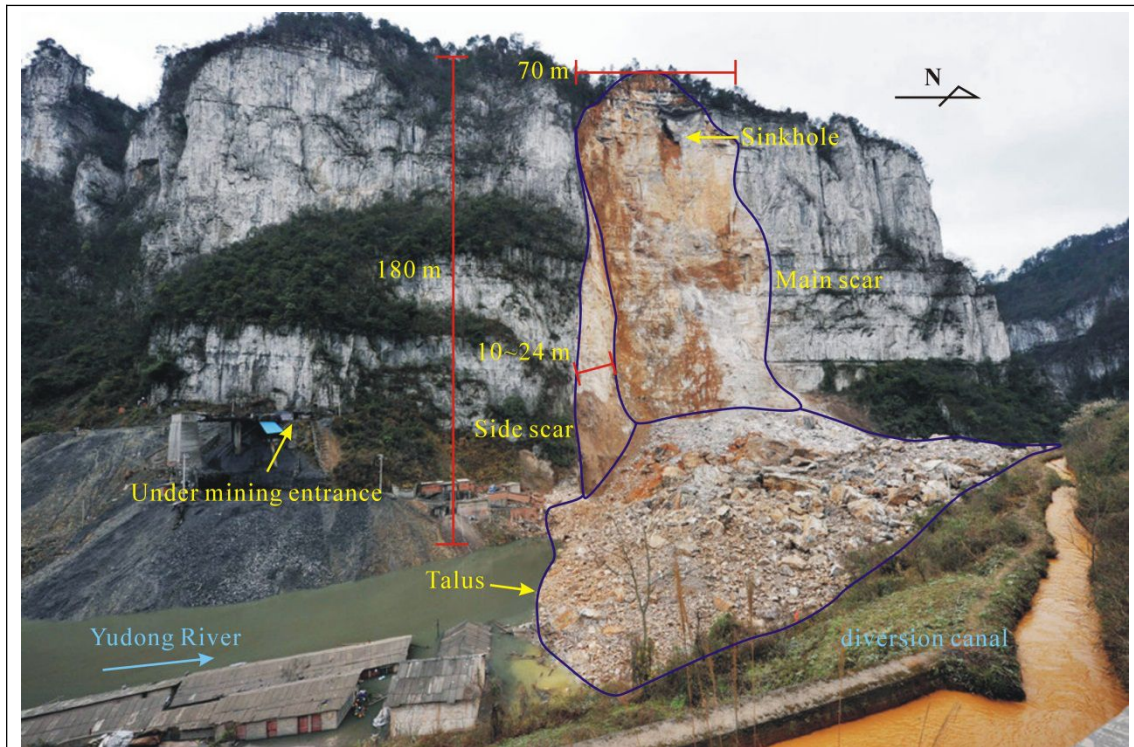


Fig. 2 Photograph showing an overview of Yudong rock slide I.

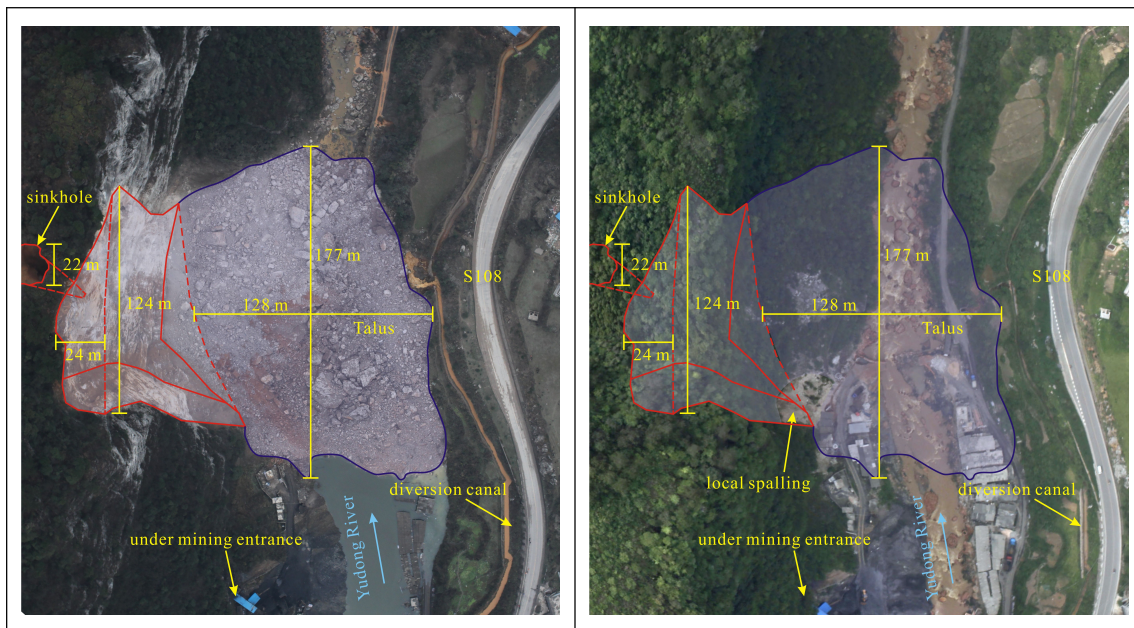
119

120 The Yudong Escarpment is about 220 m high and the slope angle is more than 80°. The steep
121 slope faces in the direction ~~SE~~100°–130°, and the dip direction is ~~NW~~325°, with slightly inclined
122 bedding. The outcrop consists of thickly bedded P_1^2 limestone and underlying P_1^1 coal measures.

123 The jointed limestone is moderately weathered, and the uniaxial compression strength of intact
124 rock reaches 30 MPa. The coal measures are composed of thickly bedded argillaceous shale and
125 coal seams. Coal extraction has been active in the soft basal unit, and the goaf is about 200 m deep
126 behind the cliff face. The Yudong Escarpment lies in the gentle eastern flank of the Yudong

127 Syncline, which strikes NNE. As a result, a set of NNE-trending joints and a conjugate set of

128 NW-trending joints are present in the rock mass. The orthogonal $130^{\circ} \angle 70^{\circ}$ and $80^{\circ} \angle 75^{\circ}$ joints
129 cut the $325^{\circ} \angle 9^{\circ}$ rock beds into prism- and tower-shaped blocks on the edge of the cliff. The
130 “2.18” Yudong rock slide originates from one of these unstable blocks with a volume of about 30
131 $\times 10^4$ m³. Several types of karst are observed in the rock slide area, including sinkholes, karst
132 tunnels, and dissolution fissures. A remote sensing image taken the day after the rock collapse
133 shows a sinkhole at the crest with a diameter of 2.2 m immediately behind the fall. The pipe flow
134 and induced groundwater dynamics acted on the unstable rock block and changed the instability.
135 However, because of abundant vegetation, the sinkhole is not visible in a previous image that was
136 taken in the summer of 2012 (Fig. 3). The intense karstic erosion of a yellowish-orange color has
137 been observed on the vertical scar. The selective karst widens and connects the pre-existing steep
138 joints so that the area of the rock bridge covers less than 30% of the main scar (Huang, 2013). The
139 directed scratches indicate the brittle failure of the rock bridges and consequent fall of the rock
140 mass. The rock slide left two scars originate from joints. The main scar is nearly parallel to the
141 cliff face and about 80 m wide. The upper part of the main scar is a sub-vertical plane, and the
142 lower parts are planar and dip out of the cliff. The conjugate side scar is about 24 m wide and
143 perpendicular to the cliff face (Fig.2).



a

b

Fig. 3 Aerial photos of Rock Slide Itaken in summer 2012 (a) and on February 19 2013 (b). The zoning of the depleted mass and talus is projected in picture (a) prior to the catastrophe. The abundant vegetation and steep terrain make it difficult to distinguish the potential failure. However, there were signs of local spalling at the toe of the cliff face (a). A 22-m-diameter sinkhole was exposed in winter, which connected with the main back scar of the rock slide (b).

144

145 Another massive rock slide (II) (Fig. 4) occurred on April 16, 2013, about 100 m away from the
 146 February 18 rock slide (I). The morphology of the vertical scar of rock slide II is similar to that of
 147 rock slide I. The lower rupture surface forms a steep and irregular scar (Fig. 5). These two rock
 148 slides have the same failure mechanism of a steep back scar separating the unstable block from the
 149 escarpment and the block breaking through the toe leading to free fall of the rock mass. The
 150 rupture surface implies a plane slide involving shear failure through the rock mass. There is little
 151 or no shear displacement along the rupture surface, and the velocity is very high. The brittle
 152 failure of the rock mass in the toe area can be explained by the brittle failure of the rock mass

153 under uniaxial compression tests. In other words, it is largely dependent on the mechanical
154 properties of the rock mass at the toe. The toe is sheared along random discontinuities of limited
155 persistence traced by the rupture surface (Fig. 6).

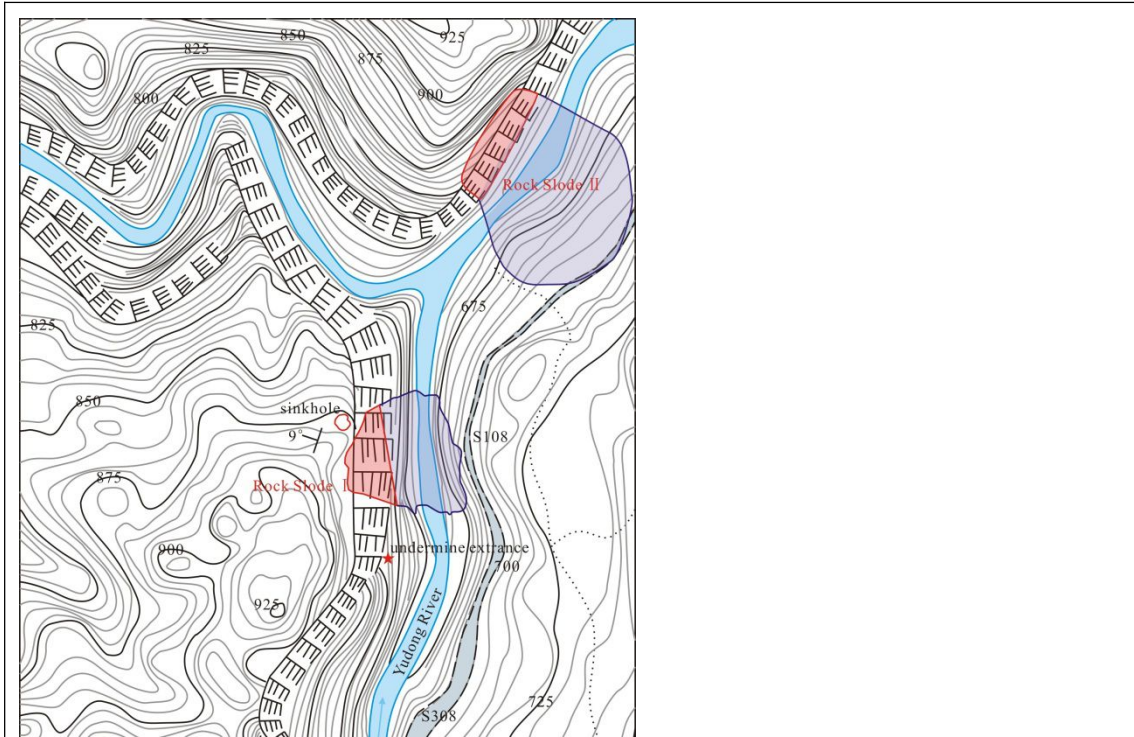


Fig. 4 Rock slide II is located north of rock slide I and has the same geological conditions, except for undermining. The volume of the talus of rock slide II is $30 \times 10^4 \text{ m}^3$. It blocked the Yudong River and covered 80 m of the S308 road.

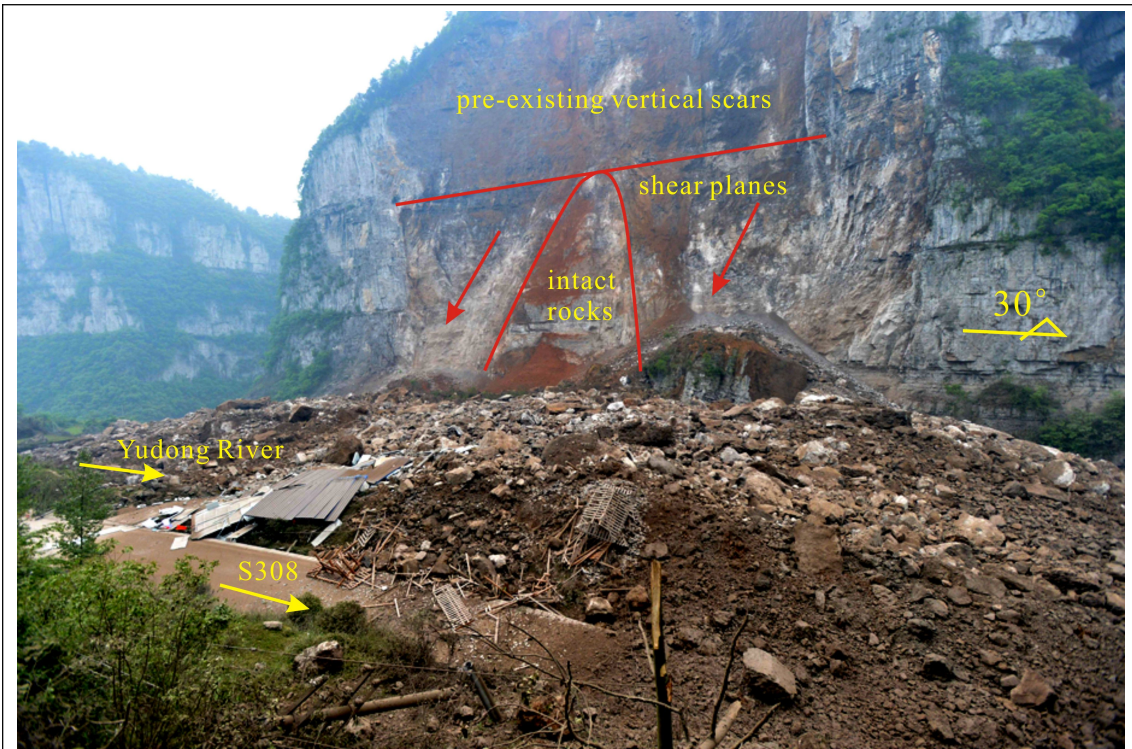


Fig. 5 Photograph showing rock slide II at Yudong. The pre-existing vertical scars are coated with karst of a yellowish-brown color, while the rupture surfaces are white and gray, indicating brittle failure and planar sliding through the limestone.

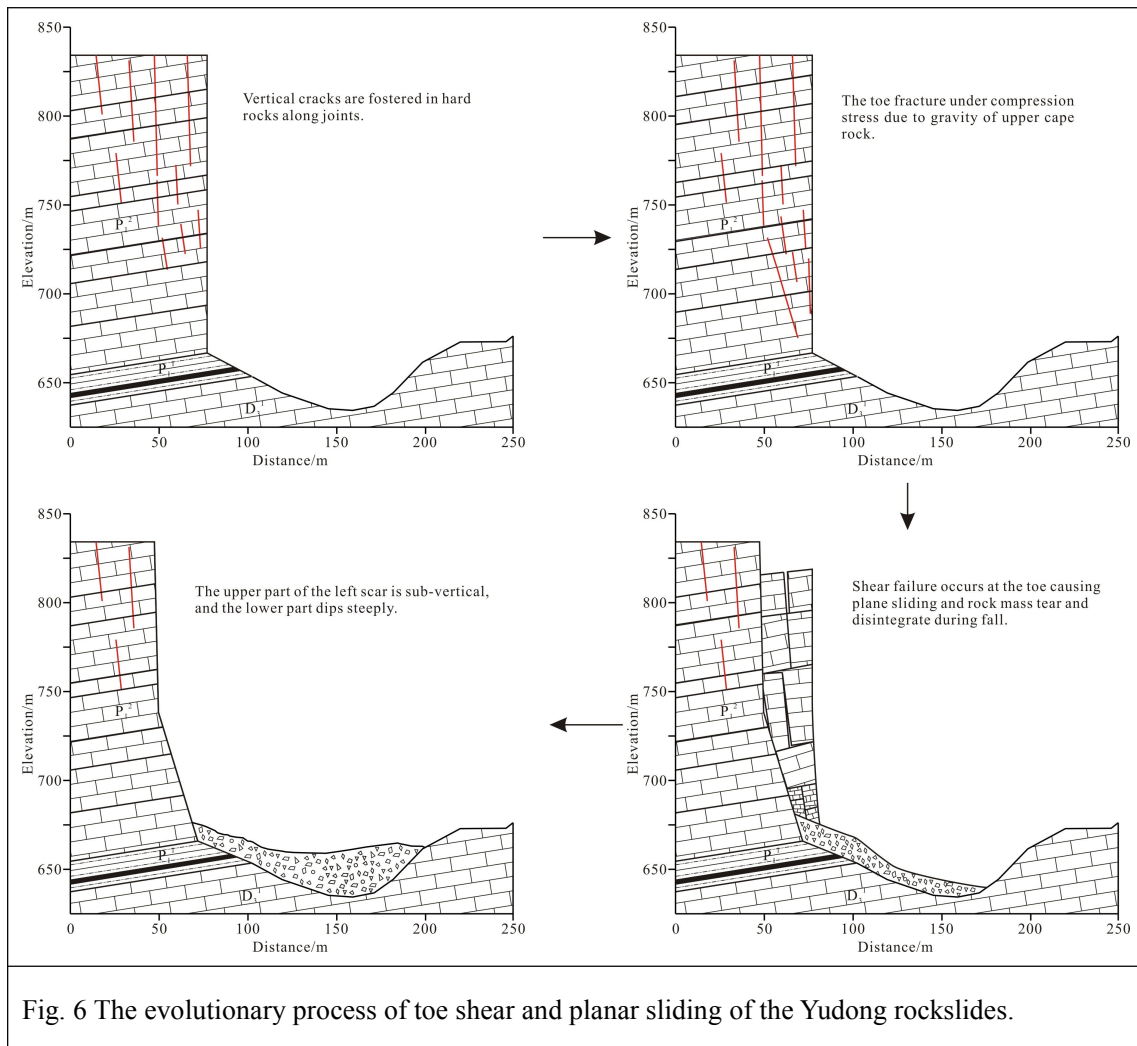


Fig. 6 The evolutionary process of toe shear and planar sliding of the Yudong rockslides.

156

157 (2) Rock collapse at Zengzi Cliff

158 Zengzi Cliff lies in the gentle and wide core of the Jinfo Mountain Syncline, Nanchuan County
 159 of Chongqing, in a “hard on soft” landform. The vertical limestone consists of two platforms
 160 separated by softer rock (Fig. 7). Two major tectonic joints in the hard rocks strike at $N40^{\circ}\text{--}50^{\circ}\text{E}$
 161 and $N30^{\circ}\text{--}50^{\circ}\text{W}$, with dip angles of $70^{\circ}\text{--}88^{\circ}$. These two sets of joints are approximately
 162 orthogonal to each other and perpendicular to bedding. The bedding trends at $300^{\circ}\text{--}305^{\circ}$ with a
 163 very low inclination ($4^{\circ}\text{--}7^{\circ}$). The upper platform is U in shape; hence, the steep slope varies from
 164 anacinal to plagioclinal and cataclinal in different parts of the edge. Beneath the cliff, S_1 silty
 165 shale forms a soft base and a gentle slope ($20^{\circ}\text{--}30^{\circ}$). Talus occurs everywhere under the cliffs,

166 indicating that cliff failure occurs as scarp retreat.

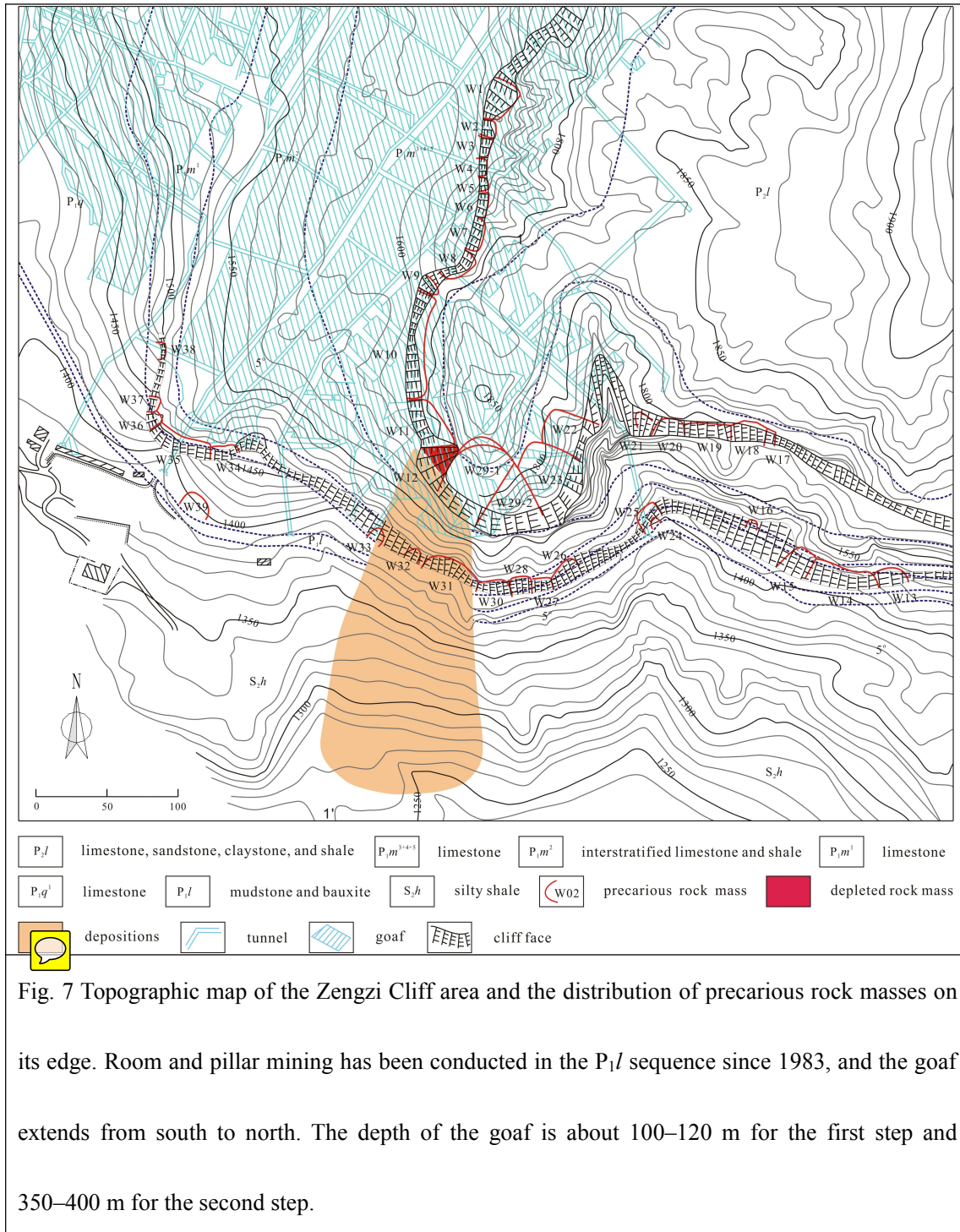
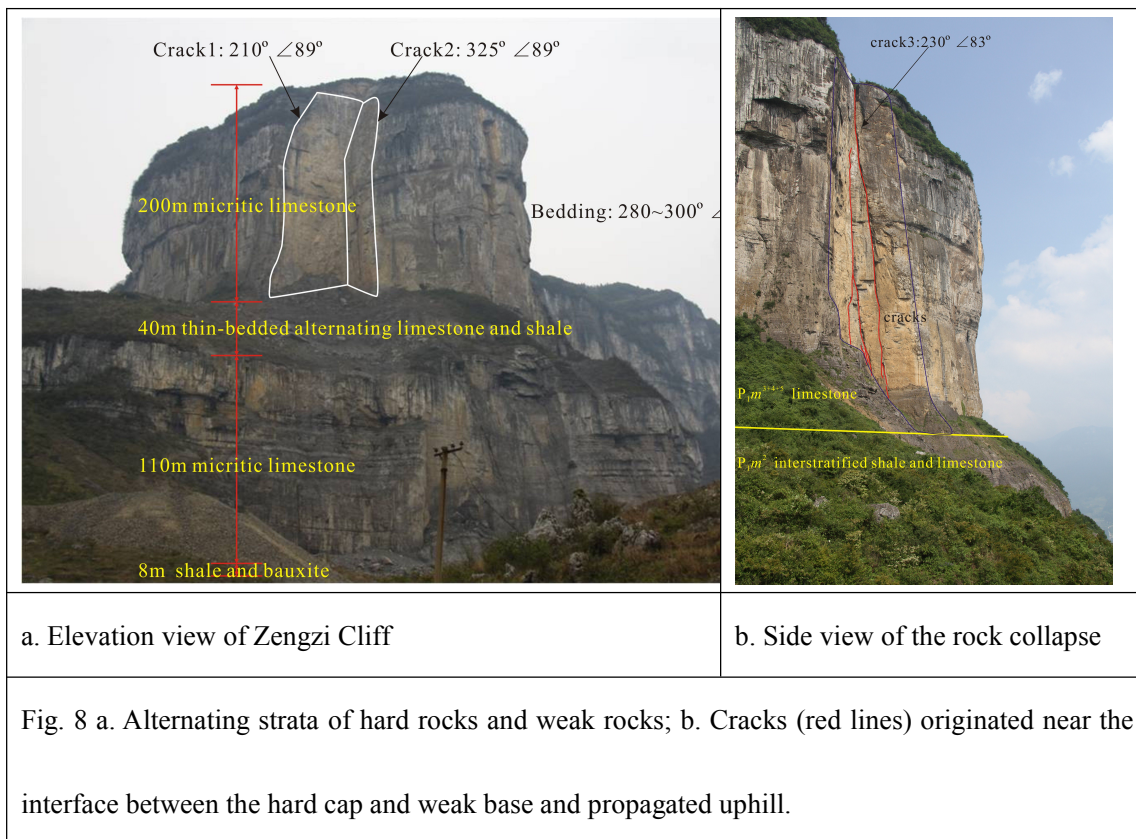


Fig. 7 Topographic map of the Zengzi Cliff area and the distribution of precarious rock masses on its edge. Room and pillar mining has been conducted in the P_1l sequence since 1983, and the goaf extends from south to north. The depth of the goaf is about 100–120 m for the first step and 350–400 m for the second step.

167

168 Rocks frequently fall in the Zengzi Cliff area. On August 12, 2004, a massive rock collapse
 169 occurred in the upper platform, which is about 200 m high (Fig. 8). The depleted mass is a prism
 170 block shaped by sub-vertical joints and bedding. Two vertical back scars and a groove surface in

171 the underlain soft strata are exposed after the collapse. Large areas of the scars are coated with
 172 karst argillaceous fillings and yellowish-orange calcite, while the rock bridge failure scars are
 173 fresh. Field investigations showed that the head scars are wide open prior to the massive collapse.
 174 Seepage forces and frost from percolating water acted on the prism block over a long time and
 175 influenced the stability; however, only karst could alter the conditions in the rock adjoining the
 176 slope by increasing the connectivity of back scars. The underlying soft strata consist of alternating
 177 beds of thin-bedded shale and medium-bedded limestone, and as a result of weathering, form a
 178 40-m-high slope.



179

180 Mining activity has been conducted for decades, but community monitoring started in 2001.

181 The opening velocity of the head scar was very slow from 2001 to 2003 (Ren, 2005). It increased

182 to 4–15 mm/10 d in the period between April and July 2004 (Fig. 9), and signs of pre-collapse,

183 (rock falls) were repeatedly observed. At that time, the government issued warnings and evacuated
 184 residents and workers. The velocity abruptly increased from August 10, and the increment reached
 185 658 mm on the last day. The process of the Zengzi rock collapse was captured on video: the tower
 186 dropped vertically and disintegrated while falling. It is unusual that the failure initiated in the
 187 bottom of the hard block rather than the underlying soft strata. The splitting of the hard rock mass
 188 at the toe led to tower collapse. The curved surface in the soft strata will have been carved by
 189 collision.

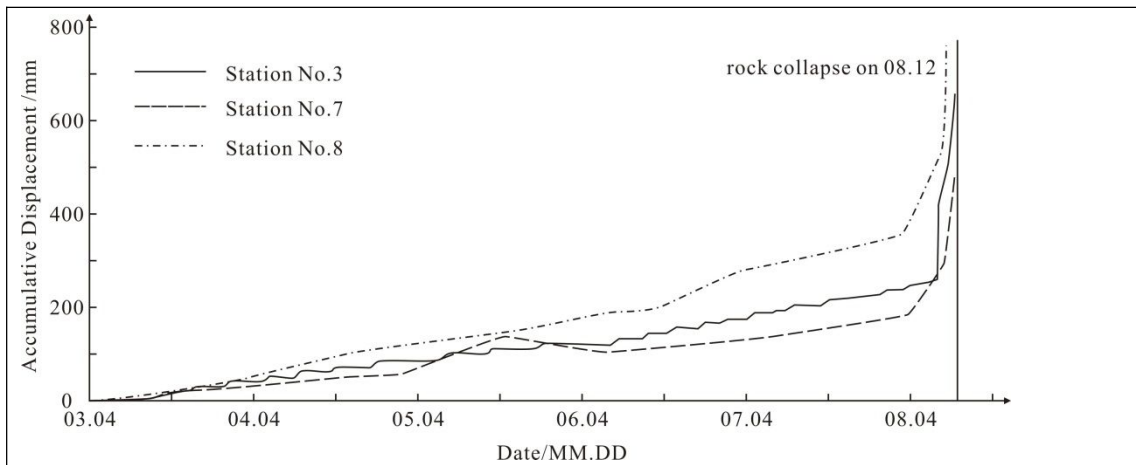


Fig. 9 Cumulative displacement of monitoring stations at the crest of Zengzi Cliff in 2004 (Ren, 2005).

190

191 Tensile splitting has been observed in uniaxial compression tests of rock samples with high
 192 brittleness and strength, such as limestone. There are several reasons why the collapse did not start
 193 with shear failure in the underlying strata. The rock mass in the bottom of the tower block is in
 194 poor condition: fractured and weathered. Drill cores obtained strongly karstic rock containing
 195 dissolution pores, caves, tufa, and calcite. The drilling also revealed at least 11 fissures, some of
 196 which were filled with yellow clay (107 Geology Team, 1995). This is because the underlying
 197 strata are low-permeability soft rocks; hence, there are steady water flows immediately above.

198 Furthermore, the soft strata are not sufficiently weak. These strata consist of interbedded thin
 199 layers of shale (0.1–0.2 m) and medium-thick limestone. The tower block could easily shear
 200 through the shale but not the intercalated limestone. Under these circumstances, tensile split
 201 failure of the tower bottom is a reasonable failure mechanism, involving compression fracturing
 202 and horizontal shearing in the shale beds (Fig. 10). Field studies and deformability tests on rock
 203 masses all around the world have demonstrated that folded and flat-lying rock masses are prone to
 204 tensile splitting near thin weak planes. Compression fracturing and tensile splitting are important
 205 failure mechanisms for sub-horizontally bedded slopes. The Zengzi cliff collapse exposed back
 206 scars in the nearby deformable rock mass, which propagated uphill (Fig. 8b), and a fractured rock
 207 mass was observed near the shale interface.

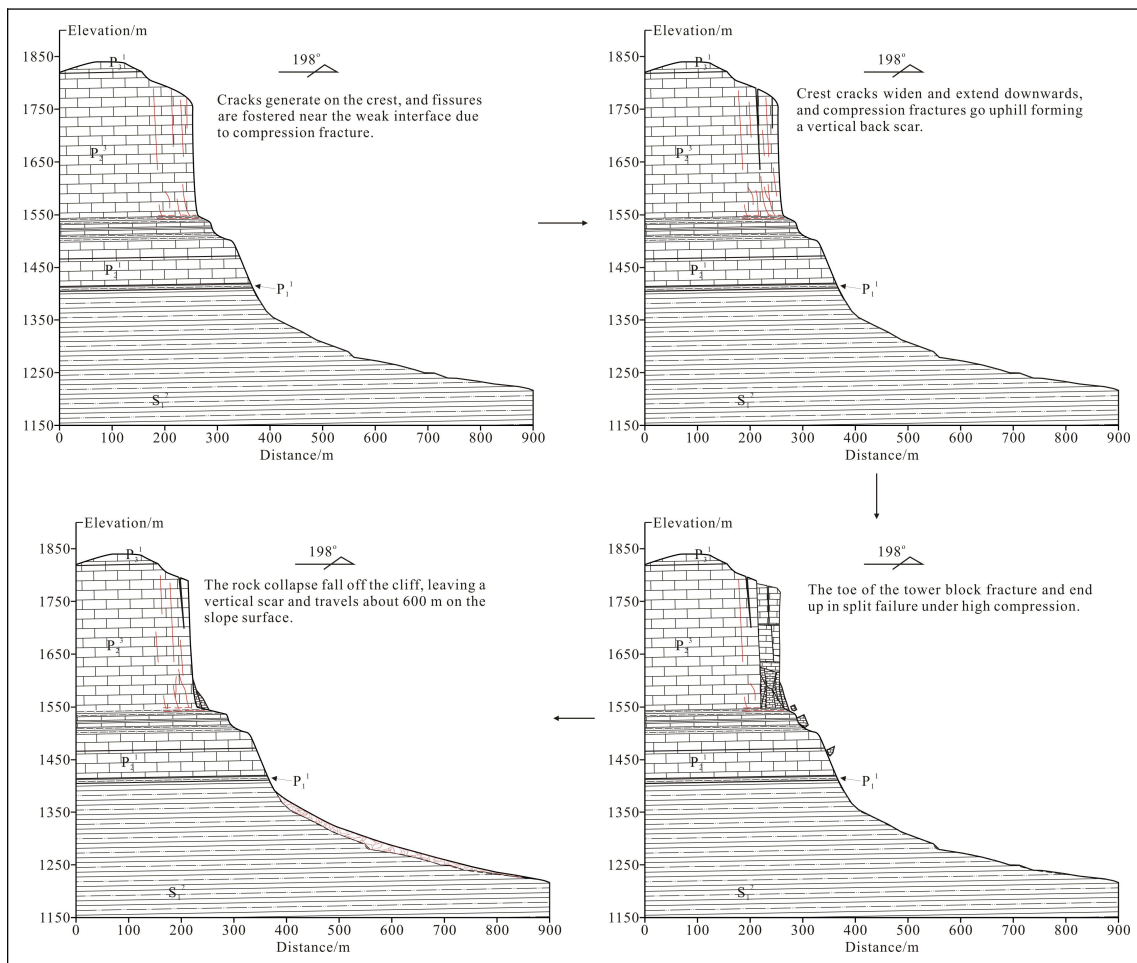


Fig. 10 Failure process of the Zengzi rock collapse, involving toe splitting and tensile failure.

208

209 **(3) Rock slump at Wangxia Cliff**

210 When the base is sufficiently weak, and there is a steep fracture separating the column from the
211 slope in the cap area, a rock slump with back-tilting mechanism is likely to occur. The Wangxia
212 Cliff failure slump mechanism involved isolated limestone block breaking through shale at the toe,
213 with rotational movement. The Wangxia Cliff is situated at the top of the right bank of the Yangtze
214 River in Wushan County of Chongqing, about 1000 m above the water level (Fig. 11). Located in
215 the flat core of the Hengshixi Fold, the bedding is slightly inclined (3° – 8°) and strikes at
216 335° – 340° , opposite to the cliff face. Interbedded shales, mudstones, and coal seams form a gentle
217 slope and separate the Upper Permian limestone into two cliff steps. A country road passes over
218 the slope below the 70–75-m high limestone escarpment, which contains several isolated slab- and
219 prism-shaped blocks. On October 21, 2010, a prism with a volume of $7 \times 10^4 \text{ m}^3$ became a rock
220 slump failure.



Fig. 11 Overview of Wangxia Cliff prior to the catastrophic rock slump. G01 represents a GPS station, and Lw02–Lw07 indicate the displacement monitoring stations. The rock slump of October 21, 2010 was controlled by vertical scars T11 and T12. The red lines represent fissures in the rock mass.

221

222 The slope movement can be traced back to June 18, 1999. Four collapsecraters and nine cracks

223 were observed in the crest area after 108.5 mm of rainfall on June 15 and 16 (Le, et al., 2011).

224 Intensive deformation began on August 21, 2010, after four days of concentrated rainfall.

225 Repeated pre-collapse signs were observed. Crown cracks widened, and new cracks occurred on

226 the crest. Rocks fell off from the cliff face and vertical scars in the rock mass. In addition, gravelly

227 soils flowed out from steep cracks at the toe. Transverse ridges and cracks were observed on the

228 country road beneath. The mass movement accelerated as a result of 70 mm of precipitation from

229 October 10 to 13. The fissures in the isolated blocks extended and widened. Rock falls became

230 more obvious both in volume and frequency. Finally, a massive rock slump occurred on October
231 21, in which the isolated prism slid downhill, breaking through the toe and leaning against the
232 back scars. The underlying weak rocks were squeezed out and scattered over the slope surface.
233 Displacement monitoring showed that the crest was dominated by subsidence, while the horizontal
234 and vertical displacements were about the same at the base. The incompetent base showed
235 horizontal movement and little subsidence. These phenomena were caused by ductile yielding and
236 rotational shearing in the incompetent base (Fig. 13). The squeezing out contributed to the uphill
237 propagation of cracks and disintegration of the mountain into slab- and prism-like blocks.

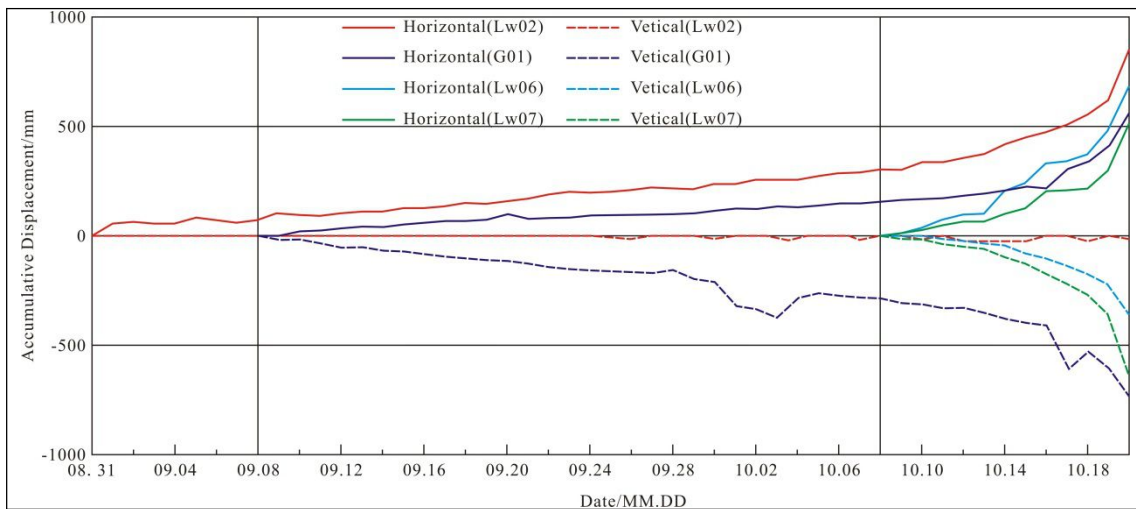


Fig. 12 Cumulative displacement at monitoring stations at the Wangxia rock slump (Le, et al., 2011).

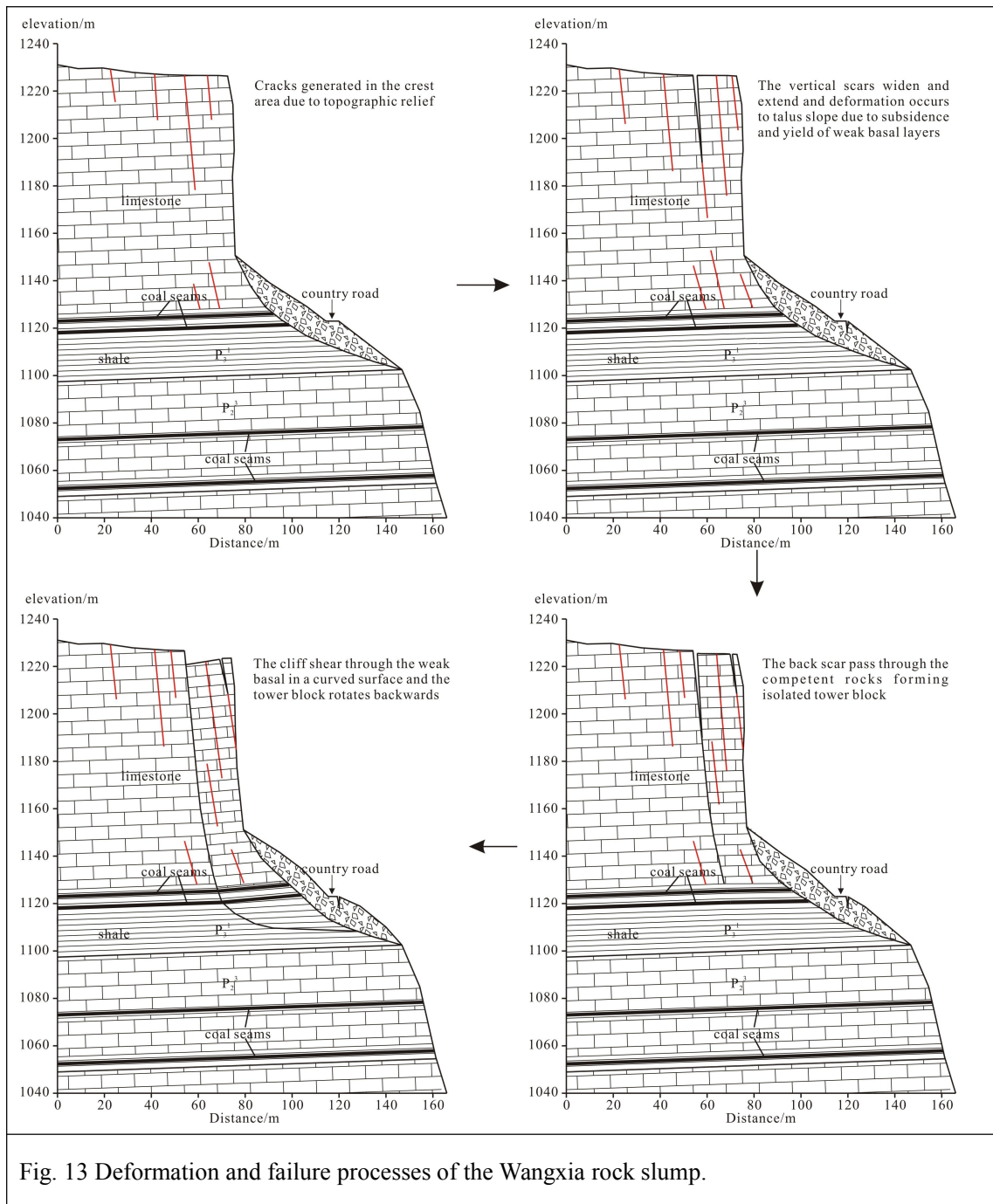


Fig. 13 Deformation and failure processes of the Wangxia rock slump.

238

239 It is worth mentioning that there is a good correlation between the acceleration of displacement
 240 and concentrated rainfall. Because of cracks and fissures in the limestone, water could easily and
 241 rapidly percolate into the weak strata. The unconfined compressive strength (UCS) of the shale
 242 shows a substantial decrease when saturated, and the softening factor is about 0.62. However,
 243 there is a 2–4 day time lag between concentrated rainfall and acceleration of displacement,

244 because the infiltration of water into poorly permeable shale takes time.

245

246 4. Numerical back-analysis

247 Numerical analysis is a sophisticated method for assessing the potential failure modes of rock

248 slopes. We use it herein to validate the cases discussed above, which show different failure

249 mechanisms for sub-horizontally bedded cliffs (compound slide, rock collapse, and rock slump)

250 and to explain the backgrounds to the slides. The computation was performed using the computer

251 program UDEC; the parameters used in the simulation are given in Table 1.

252 Table 1 Parameters used in the numerical simulation

parameter	limestone	shale		
		Rock slide	Rock collapse	Rock slump
Thickness (m)	170	20	2	20
Density(kg/m ³)	2700	2640		
Young's modulus, E(GPa)	65	5		
Poisson'sratio	0.13	0.2		
Friction angle of rock mass (°)	32	28	20	25
Cohesion of rock mass (MPa)	1.3	0.8	0.4	0.5
Tensile strength of rock mass (MPa)	0.3	0.1	0.04	0.04
Friction angle of joints (°)	30	25		
Cohesion of joints (MPa)	1.0	1		
FOS	-	1.01	1.21	1.07

253

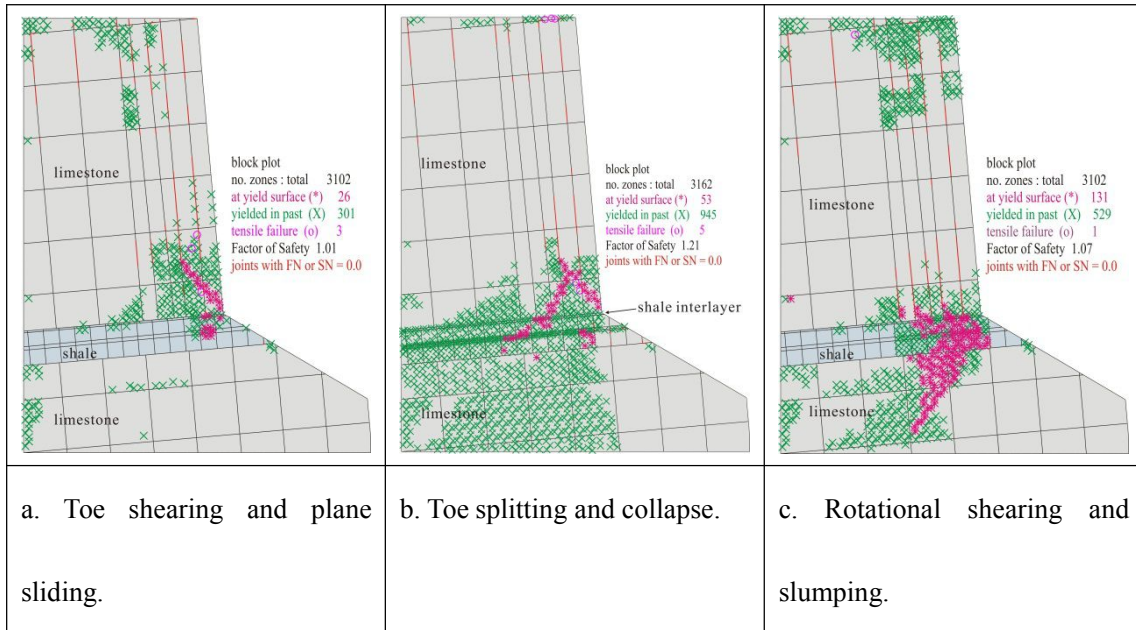


Fig. 14 Plastic state and joint opening for rockslide initiation in cliff slopes.

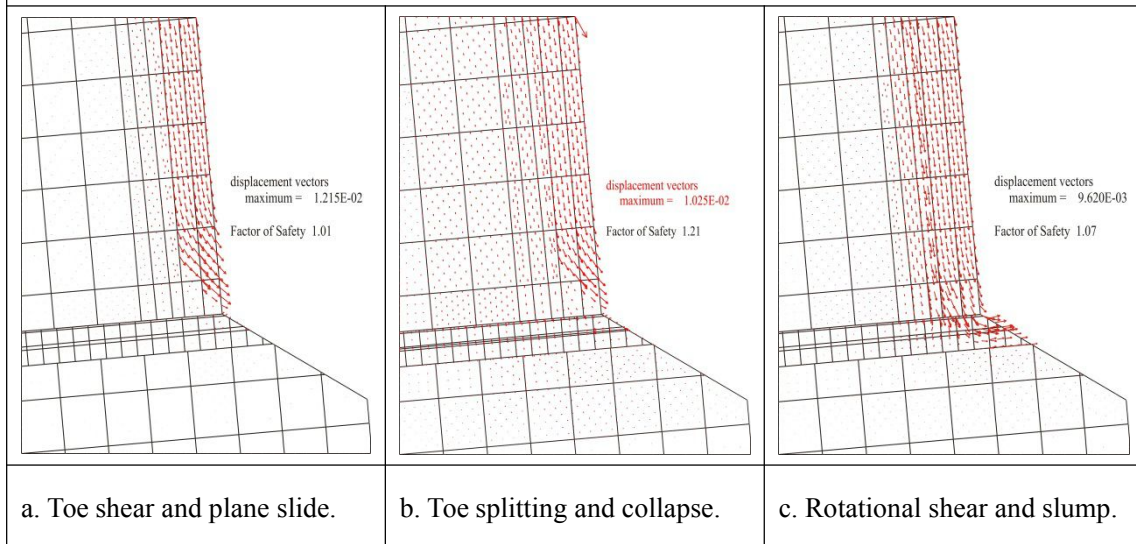


Fig. 15 Displacement vectors of the initial failures of cliff slopes.

254

255 The natural stress field is characterized by a tensile zone on the crest and stress concentration at
256 the toe. When a thick incompetent basal layers is present, the jointed slope tends to fail as a slump.

257 A yielding curved surface gradually emerges in the basal layers under long-term gravitational
258 compression of the upper cap rock. A large plastic zone is present in the weak basal layers and
259 nearby hard rock mass (Fig. 14c). The horizontal movement of the weak stratum is prominent.

260 Pre-existing joints in the hard rock mass widen upward and slip with the ductile flow of the basal
261 layers. The movement of the massive unstable rock mass is dominated by subsidence in the crest
262 area and back tilting at the toe (Fig. 15c).

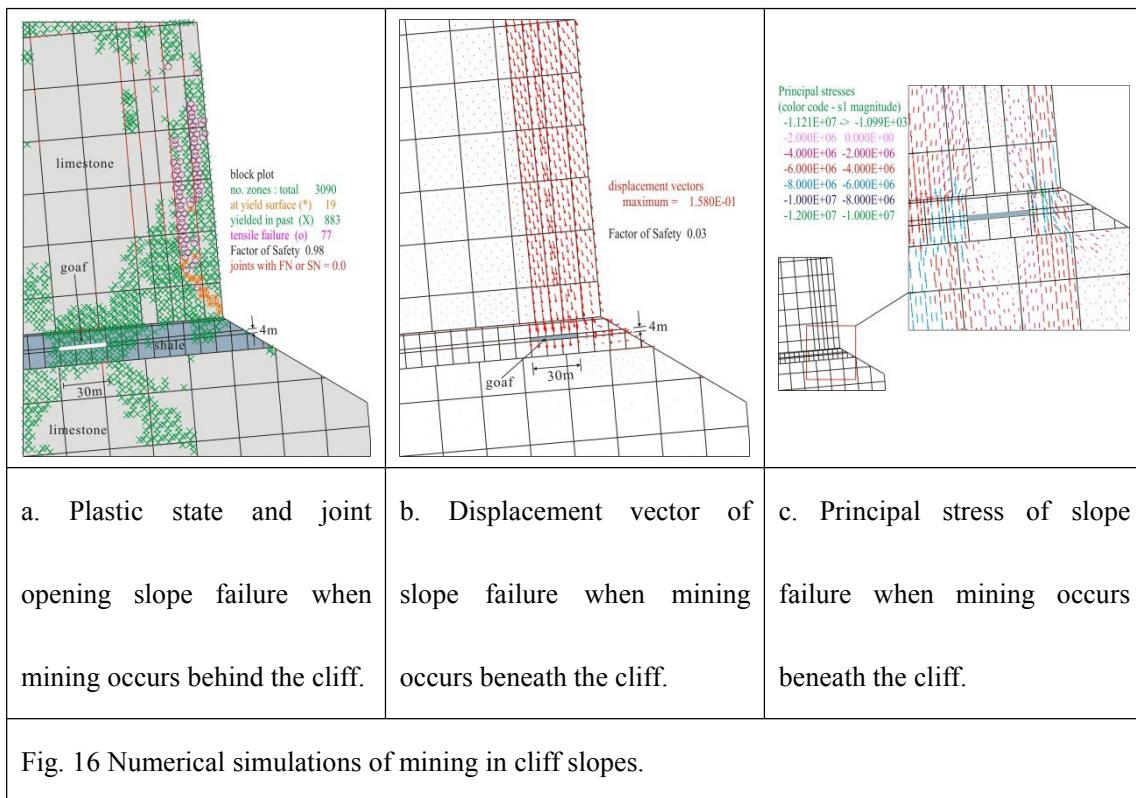
263 When the weak basal is a thin interlayer, rotational slide through the toe is unlikely to occur. The
264 horizontal shear stress determines the possibility of shear failure in the beds. For a sub-horizontal
265 bedded slope with gentle tectonic disturbance during geologic evolution, the horizontal to vertical
266 stress ratio is generally less than 1 (Zhang, et al., 1994). This indicates that it is possible for a
267 weak interlayer with a frictional angle less than 45° to shear horizontally. Under these
268 circumstances, the plastic zone ranges over the interlayer as well as the overlying competent rocks.
269 The rock mass at the toe is in a plastic state as a result of compression fractures. Two yield
270 surfaces dipping in opposite directions are formed (Fig. 14b), similar to tensile failure behavior for
271 some brittle rock samples. The displacement prior to collapse is limited, and remarkable squeezing
272 out is unlikely to be observed in the toe area (Fig. 15b).

273 A rock slide might burst out in hard rock where back scars cut through, and no discontinuities or
274 weak strata are exposed at the toe. Irregular scars caused by brittle and shear failure through rock
275 mass dip out of the cliff faces. The yield zone is mainly located at the block toe but not in the
276 underlying rocks(Fig. 14a). The fracture of the toe rock mass gives rise to joints opening
277 immediately above. Numerical computation gives a plane yield surface at the bottom of the
278 separated block, which is called a potential failure surface (Fig. 15a). A small displacement
279 appears before the outbreak of a compound slide. However, ground fractures on the crest and
280 spalling in the toe area might occur.

281

282 **5. Underground mining**

283 The failures at the three locations described above are related to large areas of mining out. Pells
 284 (2008) used a continuum 2D model to assess macro-scale movements of cliff faces caused by total
 285 extraction and proved that the steep slope tends to tilt outwards when mining occurs beneath the
 286 cliff, and extraction well behind the cliff face causes back tilt. Our similar simulations are shown
 287 in Fig. 16. The rock slide model in Fig. 14a was adopted. The roof tends to collapse, and the
 288 surrounding rocks gradually fracture. The undermining-induced subsidence of the crest causes the
 289 dilation and tensile failure of the rock mass (Fig. 16a). The FOS decreases from 1.01 to 0.98 when
 290 the underground mining is located behind the cliff face. When the extraction is directly beneath
 291 the cliff, the rock mass is subjected to a small constraint; hence, cliff failure break-out through the
 292 fractured rock mass between the goaf and open face is feasible (Fig. 16b). The maximum principal
 293 stress on both sides of the goaf increases while that of the overlying rocks decreases (Fig. 16c).



295 **6. Conclusions**

296 In this study, three different examples of failure in sub-horizontally bedded limestone cliffs are
297 discussed. The failures are characterized by pre-existed vertical joints passing through thick
298 limestone. The Yudong rock slide originated in a limestone cliff edge and left a moderately
299 inclined rupture plane, implying shear failure through the hard rock. Rock collapse caused by
300 compression fracture and tensile splitting of the rock mass near the interface between the hard cap
301 and weak stratum occurred at Zengzi Cliff. The Wangxia cliff failure showed a slow rock slump
302 sheared through the underlying incompetent rock mass along a curved surface. The mechanism of
303 toe breaking mainly depends on the strength characteristics of the rock mass.

304 Considering that the rock mass near the cliff face is not laterally constrained, it is reasonable to
305 assume that there is a massive UCS failure at the toe of the vertical tower and slab blocks.
306 Some failure characteristics of jointed rock mass in in situ UCS tests have been observed all
307 around the world, for both shear and tensile failure. Of special concern is tensile failure in
308 horizontally bedded rock masses with interlayers. Compression fractures emerge near the
309 interfaces and form vertical slabs, which eventually split. Another possibility is squeezing out of
310 weak interlayers as a result of compression fracture, causing the hard rock nearby to yield to
311 tensile stress and disintegrate. It is worth noting that the UCS of the rock mass in compression
312 fracturing is much lower than that of intact rock. A criterion based on horizontal shear failure
313 along weak interlayers and the UCS ratio of the cap and underlying rock masses could be used to
314 assess the failure mode of tower and slab blocks on cliff edges.

315

316 **Acknowledgments**

317 This work was carried out with financial support from the China Geological Survey (No.
318 12120114079101), the Ministry of Science and Technology of the People's Republic of China (No.
319 2012BAK10B01) and the National Natural Science Foundation of China (No. 41302246).

320

321 **References**

322 107 Geology Team of Sichuan Geology and Mineral Bureau. (1995). Geology Survey Report
323 on Bauxite Deposit of Loujiashan in Nanchuan, Sichuan (in Chinese).

324 Abele, G. (1994). Large rockslides: their causes and movement on internal sliding planes.
325 Mountain Research and Development, 14(4): 315-320.

326 Altun A.O., Yilmaz I., Yildirim M. (2010). A short review on the surficial impacts of
327 underground mining. Sci Res Essays, 5(21), 3206-3212.

328 Ding W.W, Yu Y.Z, Deng W.L., et al.(1990). Stability analysis of reservoir bank in Three
329 Gorges of Yangtze River. Center of hydrological and engineering geology, Ministry of Geology
330 and Mineral Resource, Chengdu: 7-8. (in Chinese)

331 Embleton-Hamann C. (2007). Geomorphological hazards in Austria. Geomorphology for the
332 Future, Innsbruck University Press, Innsbruck, 33-56.

333 Hungr O., Evans S.G. (2004). The occurrence and classification of massive rock slope failure.
334 Felsbau, 22(2), 16-23.

335 Huang R.Q. (2013). Mechanisms of large-scale landslides and pre-recognition. Key note on
336 the Six National Academic Conference of Geological Hazard. April 11-12, 2013. Beijing, China.

337 Kay D., Barbato J., Brassington G., et al. (2006). Impacts of Longwall Mining to Rivers and
338 Cliffs in the Southern Coalfield. In Aziz N. (ed), Coal 2006: Coal Operators' Conference,

339 University of Wollongong & the Australasian Institute of Mining and Metallurgy, 2006, 327-336.

340 Le Q.L., Wang H.D., Xue X.Q., et al. (2011). Deformation monitoring and failure mechanism
341 of Wangxia Dangerous Rock Mass in Wushan County. *Journal of Engineering Geology*,
342 19(6):823-830.

343 Lollino P., Martimucci V., Parise M. 2013. Geological survey and numerical modeling of the
344 potential failure mechanisms of underground caves. *Geosystem Engineering*, vol. 16 (1): 100-112

345 Marschalko M., Yilmaz I., Bednárík M., et al. (2012). Deformation of slopes as a cause of
346 underground mining activities: three case studies from Ostrava–Karviná coal field (Czech
347 Republic). *Environmental monitoring and assessment*, 184(11): 6709-6733.

348 Parise M. (2008) Rock failures in karst. In: Chen ZY, et al (eds) *Landslides and Engineered*
349 *Slopes*. Proc. 10th Int. Symp. on Landslides, Xi'an (China), June 30–July 4, 2008, 1, pp 275-280

350 Parise M. (2010). Hazards in karst. In *Proceedings International Interdisciplinary Scientific*
351 *Conference “Sustainability of the Karst Environment. Dinaric Karst and Other Karst Regions.”*:
352 *Series on Groundwater*. IHP-UNESCO, Plitvice Lakes, Croatia (pp. 155-162).

353 Pells P.J.N. (2008). Assessing parameters for computations in rock mechanics. In Potvin Y,
354 Carter J., Dyskin A., et al (eds), *Proceedings First Southern Hemisphere International Rock*
355 *Mechanics Symposium (SHIRMS)*, 1:39-54.

356 Palma B., Parise M., Reichenbach P., et al. 2012. Rock-fall hazard assessment along a road in
357 the Sorrento Peninsula, Campania, southern Italy. *Natural Hazards*, 61 (1): 187-201.

358 Rainer P., Martin B., Rudolf H., et al. (2005). Geomechanics of hazardous landslides. *Journal*
359 *of Mountain Science*, 2(3), 211-217.

360 Ren Y.R., Chen P., Zhang J., et al. (2005). Early-warning analysis on the rockfall for

361 Zengziyan W12# dangerous rock mass in Nanchuan City of Chongqing. *The Chinese Journal of*
362 *Geological Hazard and Control*, 16(2):28-31

363 Rohn J., Resch M., Schneider H., et al. (2004). Large-scale lateral spreading and related mass
364 movements in the Northern Calcareous Alps. *Bulletin of Engineering Geology and the*
365 *Environment*, 63(1), 71-75.

366 Ruff M., Rohn J. (2008). Susceptibility analysis for slides and rockfall: an example from the
367 Northern Calcareous Alps (Vorarlberg, Austria). *Environmental geology*, 55(2), 441-452.

368 Santo A., Del Prete S., Di Crescenzo G., Rotella M. (2007). Karst processes and
369 slopeinstability: some investigations in the carbonate Apennine of Campania (southern Italy).
370 In:Parise M, Gunn J (eds) *Natural and Anthropogenic Hazards in Karst Areas:*
371 *Recognition,Analysis and Mitigation*. Geol. Soc. London, sp. publ. 279: 59–72

372 Tang F.Q. (2009). Research on mechanism of mountain landslide due to underground mining.
373 *Journal of Coal Science and Engineering (China)*, 15(4):351-354.

374 Von Poschinger, A. (2002). Large rockslides in the Alps: A commentary on the contribution
375 of G. Abele (193 7-1994) and a review of some recent developments. In: Stephen G Evans, et
376 al.(eds), *Catastrophic Landslides: Effects, Occurrence, and Mechanisms*,:237-255.

377 White E., White W. (1969). Processes of cavern breakdown. *Bull. Natl. Speleol. Soc.*
378 31(4):83–96

379 Zhang Z.Y., Wang S.T., Wang L.S.(1994). *Principle of Engineering Geology Analysis*. China
380 *Geology Press, Beijing: 66*